Retraction

Retracted: Complex Behavior of Droplet Transfer and Spreading in Cold Metal Transfer

Shock and Vibration

This article has been retracted by Hindawi following an investigation undertaken by the publisher [1]. This investigation has uncovered evidence of one or more of the following indicators of systematic manipulation of the publication process:

(1) Discrepancies in scope

(2) Discrepancies in the description of the research reported

(3) Discrepancies between the availability of data and the research described

(4) Inappropriate citations

(5) Incoherent, meaningless and/or irrelevant content included in the article

(6) Manipulated or compromised peer review

The presence of these indicators undermines our confidence in the integrity of the article's content and we cannot, therefore, vouch for its reliability. Please note that this notice is intended solely to alert readers that the content of this article is unreliable. We have not investigated whether authors were aware of or involved in the systematic manipulation of the publication process.

Wiley and Hindawi regrets that the usual quality checks did not identify these issues before publication and have since put additional measures in place to safeguard research integrity.

We wish to credit our own Research Integrity and Research Publishing teams and anonymous and named external researchers and research integrity experts for contributing to this investigation.

The corresponding author, as the representative of all authors, has been given the opportunity to register their agreement or disagreement to this retraction. We have kept a record of any response received.

References

[1] S. Yang, Y. Xing, F. Yang, and J. Cao, "Complex Behavior of Droplet Transfer and Spreading in Cold Metal Transfer," *Shock and Vibration*, vol. 2020, Article ID 6650155, 11 pages, 2020.

Research Article

Complex Behavior of Droplet Transfer and Spreading in Cold Metal Transfer

Shuai Yang [ID], Yanfeng Xing [ID], Fuyong Yang [ID], and Juyong Cao [ID]

School of Mechanical and Automotive Engineering, Shanghai University of Engineering Science, Shanghai 201620, China

Correspondence should be addressed to Yanfeng Xing; smsmsues@163.com

In intelligent manufacturing, an intelligent control method of welding process is an important process of intelligent welding manufacturing technology (IWMT). Metal transfer is a key factor to control the welding process. Metal transfer and droplet spreading are of vital importance for welding formation. A new theoretical model of cold metal transfer (CMT) in short-circuit transfer mode is proposed in this paper. In this model, the CMT welding process is regarded as a continuous process of arc heating, mass transfer, short-circuit, and spreading, and the relations between these processes are analyzed. The calculation equations used by the model can analyze the welding formation clearly and simplify the complex welding process into continuous physical behavior. The predicted welding width shows good agreement with the measurement results. The mechanism of increased welding width is also comprehensively analyzed. Results have a certain guiding effect on aluminum alloy welding process control.

1. Introduction

In intelligent manufacturing, a weld controller is a typical system of the intelligent welding manufacturing system [1]. Intelligent control of welding dynamic process is one of main problems of intelligent welding technology. One of problems in intelligent control of welding dynamic process is welding pool dynamic process [2]. The short-circuit transfer in the metal transition is controlled through traditional MIG (metal inert gas)/MAG (metal active gas) welding to control the heat input and reduce the welding defects. Cold metal transfer (CMT) is an improvement of short-circuit transfer in GMAW (gas-metal arc welding) process, which has the characteristics of low splash and low-heat input. CMT allows a better microstructure to be obtained than MIG. Feng et al. [3] carried out experiments through CMT technology to weld a 1 mm thick pure aluminum alloy with minimal deflection. Lei et al. [4] welded a 1 mm thick AA6061-T6 by using three welding arc modes of standard, pulsed, and CMT. They found that CMT arc mode produced the fewest welding defects. Cao et al. [5, 6] joined 1.0 mm thick AA6061-T6 to 1.0 mm thick galvanized mild steel using the cold metal transfer method, and the welded

joint strength can meet the requirements. These studies confirm that CMT is superior to MIG/MAG in thin-plate welding and dissimilar metal welding. CMT can effectively control the heat affected zone (HAZ) and enhance the weldability of thin metal plates and dissimilar metals.

To ensure the formation of welding, scholars have focused on optimization of CMT welding parameters. Wang et al. [7] studied the influences of parameters such as boost current, arcing current, breaking current, boosting voltage, and wire moving speed in CMT welding on the CMT boosting phase, arcing phase, and short-circuit phase. Chen et al. [8] analyzed the effects of CMT current waveform on welding formation. Kumar [9] investigated the effect of welding current and welding speed on welding formation, dilution, and contact angle during cold metal transfer (CMT) process These studies investigated the control of the welding formation through experiments, but the reasons for the changes in the welding formation were not explained theoretically.

Metal droplet behavior has been a largely underexplored domain. Few theoretical models can describe the relationship between metal droplet behavior and welding formation in the CMT process. Most studies on welding formation

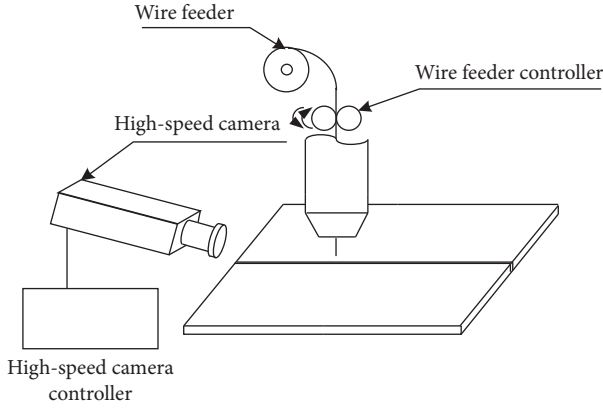

Figure 1: Welding schematic.

Figure 2: The size of workpiece.

separate from the electrode, then drip into the molten pool, and finally solidify to form a weld to join the metals together.

In the GAMW process, different metal transfer modes can be controlled by current and are affected by wire materials, shielding gas, and process parameters. In the natural state, metal transfer modes can be classified into contact transfer and free-flight transfer. In the free-flight transfer, the droplet is affected by external force and naturally separated from the wire electrode. In this case, arc welding can be divided into the following stages according to the metal transfer behavior: droplet growth stage, droplet separation stage, and droplet spreading stage. In short-circuit transfer, the metal droplet is expanded to the molten pool before separation, and the metal droplet comes in contact with the liquid molten pool. The metal behavior is mainly in the following four stages: droplet growth stage, short-circuit stage, droplet separation stage, and droplet spreading stage.

For some special welding requirements, droplet transfer can be controlled. For example, thin-plate welding and dissimilar metal welding need low-heat input. During the short-circuit transfer mode, droplet slash and heat input become easier to control due to physical contact between the metal droplet and the molten pool. Therefore, some controlled short-circuit transfer technologies have been

developed based on short-circuit transfer technology, as reported by Norrish et al. [22].

CMT is related to controlled metal transfer. CMT is based on short-circuit transfer and controls the movement of the wire electrode. The CMT droplet transfer is shown in Figure 3. The transfer of droplet occurs during the short-circuit stage of the welding process cycle, and the movement of the wire helps the droplet transfer into the molten pool. In the necking stage, the movement of the wire is used to assist the separation of the droplet from the wire electrode. In CMT, the controlled short-circuit transfer can reduce the current heat input and the droplet shock, as reported by Pang et al. [23].

3.2. The Growth of Droplet. Welding parameters on CMT mainly affect welding wire melting and droplet transfer. The adjustment of parameters will affect the growth and separation of droplets. In the CMT welding process, the behavior of the metal transfer is influenced by current. In the droplet growth phase, the arc ignites the wire electrode, which is affected by arc heat and Joule heat. The welding wire melts to form droplets at the electrode.

Joule heat can be calculated by

$$Q_J = \int_V \rho(T)I^2 dV = \overline{\rho} A L I^2, \tag{1}$$

where $\overline{\rho}$ is the average electrical resistivity, L is the electrode extension, and A is the cross sectional area of the electrode. Arc heat can be obtained by

$$Q_A = \left(\frac{3}{2}\frac{kT_a}{e} + V_a + \Phi\right)I, \tag{2}$$

where k is the Boltzmann constant, e is the elementary charge, V_a is the voltage value that characterizes the wire heating by the arc, T_a is the average arc temperature, and Φ is the work function of the electrode material.

Assuming that all heat input is used to melt the wire, the melting rate is the total heat input by the system divided by the heat required to melt the unit mass of the materials, as reported by Planckaert et al. [21]:

$$\frac{dm_R}{dt} = \frac{\overline{\rho} A L I^2 + ((3/2)(kT/e) + V_a + \Phi)I}{\int_{T_1}^{T_2} C_p dT + \Delta H_T + \Delta H_M}, \tag{3}$$

where ΔH_T is the heat of crystalline transition and ΔH_M is the heat of fusion. T_W is the wire temperature. The melting rate can be further simplified as a function of welding current, as reported by Modenesi et al. [24]:

$$\frac{dm_R}{dt} = \dot{m}_R = M_R = \alpha I + \beta l_s I^2,$$

$$m_R = \frac{4}{3}\pi R^3 \rho, \tag{4}$$

where M_R is the wire melting rate, α is the arc heat coefficient, β is the Joule heat coefficient, m_R is the droplet mass, R is the droplet radius, and ρ is the mass density of metal

TABLE 1: Experimental parameters used in CMT welding.

Test code	Wire feed speed (m/min)	Welding speed (m/min)	Shielding gas (vol.% Ar)
1	3.0	0.48	99.995
2	3.5	0.48	99.995
3	4.0	0.48	99.995
4	4.5	0.48	99.995
5	5.0	0.48	99.995
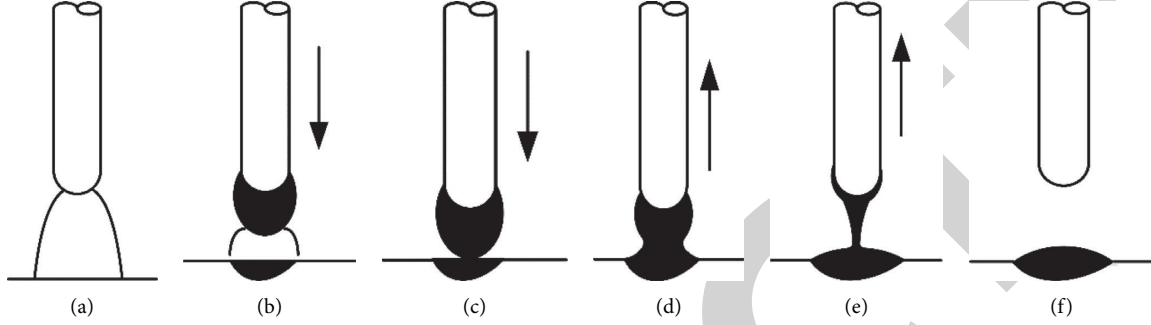
FIGURE 3: Short-circuit transfer in CMT.

droplet. These values of physical parameters are listed in Table 2.

The wire feed speed is not completely equal to the melting caused by the welding current. The wire feed system controls the wire feed speed. When the wire feed speed increases, it feeds downward, and when it decreases, it draws back:

$$\frac{dl_s}{dt} = v_{wfd} - \frac{dm}{\pi \rho r^2 dt},$$ (5)

where r is the electrode radius, and v_{wfd} is the wire feed speed. When the electrode wire feeding is higher than the wire melting rate, the droplet grows and the wire electrode feed motion helps droplets contact the weld pool.

The growth and separation of droplets can be described by establishing a dynamic model of CMT. The state of the droplets during the transition can be studied using a dynamic model to investigate analyze the influence of the movement of droplet transfer on the melting width of the molten pool.

Assuming that the droplets formed by the welding are spherical droplets, the molten material from the electrodes enters the droplets at a velocity. During the growth phase of the droplet, according to the conservation of momentum, the mass of the droplet changes from m_1 to $m_1 + dm$, and the speed of the droplet relative to the system changes from v_1 to $v_1 + dv$, as shown in Figure 4, where u_1 is the speed of the fluid mass change relative to the droplet, that is, the speed at which the molten wire flows into the droplet.

The growth stage of the droplet can be regarded as a variable mass system. The system meets the momentum theorem. According to the momentum theorem, the liquid metal melted flows into the droplet, and the mass of the droplet increases. The droplet is affected to an external force, and the system momentum changes:

TABLE 2: Physical parameter values used for calculations.

Properties (units)	Values
ρ Density (kg·m^{-3})	2700
A Area of the electrode (mm^2)	1.44
V_a Arc voltage (V)	18
α Arc heating parameter (kg/As)	7.992×10^{-11}
β Joule heating parameter (kg/mA^{2}s)	1.252×10^{-11}
γ Surface tension (N/m)	1.2
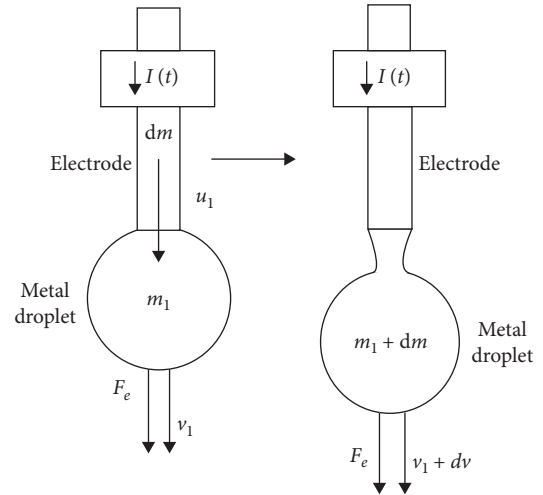
FIGURE 4: Variable mass system of droplet growth.

$$dp = p_2 - p_1.$$ (6)

The impulse of the combined external force on an object is equal to the increase in its momentum, and the equation can be written as

$$F_e dt = (m_1 + dm)(v_1 + dv) - (m_1 v_1 + u_1 dm),$$

$$F_e dt = m_1 v_1 + v_1 dm + m_1 dv + dm dv$$
$$- v_1 dm - u_1 dm - m_1 v_1,$$

$$F_e dt = m_1 dv + dm dv - u_1 dm,$$

$$F_e dt + u_1 dm = (m_1 + dm)dv.$$

$$(7)$$

The conservation of momentum for the metal droplet can be written as

$$m(t)\frac{dv}{dt} = F_e + u_1 \frac{dm}{dt}, \tag{8}$$

where $m(t) = m_R = \int M_R dt$, F_e is the external forces, and $u_1 = (M_R / 4\pi\rho r^2)$.

The external forces that affect droplets are Lorentz force, surface tension, and gravitational force, as reported by Ersoy et al. [17]. In the CMT process, the electrode feed force also needs to be considered, as shown in Figure 5. In the short-circuit stage, the wire feeding system controls the wire drawing to assist the liquid bridge break and metal transfer to the molten pool:

$$F_{em} = \frac{\mu_0}{4\pi}I^2 P,$$

$$F_s = 2\pi R\gamma,$$

$$F_g = \frac{4}{3}\pi R^3 \rho g,$$

$$P = \left[\ln\frac{R\sin\theta_z}{r} - \frac{1}{4} - \frac{1}{1-\cos\theta_z} + \frac{2}{(1-\cos\theta_z)^2}\ln\frac{2}{1+\cos\theta_z}\right],$$

$$(9)$$

where γ is the surface tension coefficient, F_{em} is the Lorentz force, F_s is the surface tension, F_g is the gravitational force, F_f is the electrode feed force, μ_0 is the permeability of free space, R is the droplet radius, r is the electrode radius, and θ_z is the conduction zone radius.

In this model, the droplet displacement caused by the increase in the droplet mass is small, so the liquid bridge shrinkage is ignored in the growth stage. In this case, the liquid bridge radius is equal to the wire radius. In the droplet growth stage, the wire feed force is 0; when the current level is high, external forces will change the droplet transfer mode, which becomes a combination of short-circuit transitions and other transitional forms.

When droplet transfer occurs, the droplet transfer is mainly realized by electrode feeding, as shown in Figure 6. In thin-plate welding, less current is required, the external forces are smaller, the droplets are always attached to the wire electrode, and the transition of the droplet to the molten pool requires electrode movement.

Short-circuit transfer is affected by wire feed and droplet size. As shown in Figure 7, d is the initial distance between the welding wire and the molten pool, the wire electrode length is l_w, Δl_w is the amount of change in wire length, the arc length is l_a, the distance between the droplet and the wire electrode is d_w, and the displacement of the droplet is $D(t)$:

$$D(t) = R(t) + d_w + \Delta l_w. \tag{10}$$

When the value of $D(t)$ increases to be equal to the value of d, a short-circuit transfer occurs, and the condition of short-circuit is

$$D(t) = d. \tag{11}$$

In the short-circuit stage, the wire feeds and contacts the molten pool, and the arc length is 0. The radius of the droplet when a short-circuit transition occurs is recorded as R_i, which is used for subsequent calculations.

Equations (8) and (10) can be combined to obtain the radius of droplet and the displacement of electrode. The calculation results are shown in Figure 8, from which the motion of the droplet can be analyzed.

3.3. Separation of Electrode and Metal Droplet. When the wire is pumped back, the CMT process enters into the necking stage. As shown in Figure 9, when the droplet starts to contact the surface of the base material, the meniscus liquid surface is formed. In this stage, the electrode and the molten pool are connected by a metal liquid bridge.

As the wire is pumped back, the liquid bridge begins to shrink. According to the research of Planckaert, the pressure of the liquid bridge is calculated by

$$P_B = \frac{\mu_0 I^2}{8\pi^2 R_1^2} + \gamma\left(\frac{1}{R_1} + \frac{1}{R_2}\right). \tag{12}$$

When the value of P_B is greater than 0, the liquid bridge is broken, where γ is the surface tension of the liquid bridge. According to the momentum theorem of the variable mass system, the residual mass remaining on the wire electrode can be obtained, which will not be further discussed in this paper.

The flow velocity of the metal bridge flowing into the molten pool surface is calculated by

$$v = \sqrt{\frac{2}{\rho}(P_B + \rho gh)}, \tag{13}$$

where h is the distance from the center of liquid bridge to the surface of molten pool, which is affected by the wire extension.

3.4. The Spreading of Metal Droplet on the Surface of the Workpiece. The droplet that transitions into the molten pool will deform quickly, and in this stage, the motion of the droplet can be simplified as droplet spreading, as reported by Sivakumar et al. [25].

The droplet has an initial velocity that strikes the workpiece. In the CMT process, the droplet is always attached to the wire electrode when impacting the workpiece. Due to the influence of short-circuit transfer, the droplet is not affected by the acceleration of gravity before contacting the workpiece surface. The initial velocity of the droplet is equal to the wire feed speed.
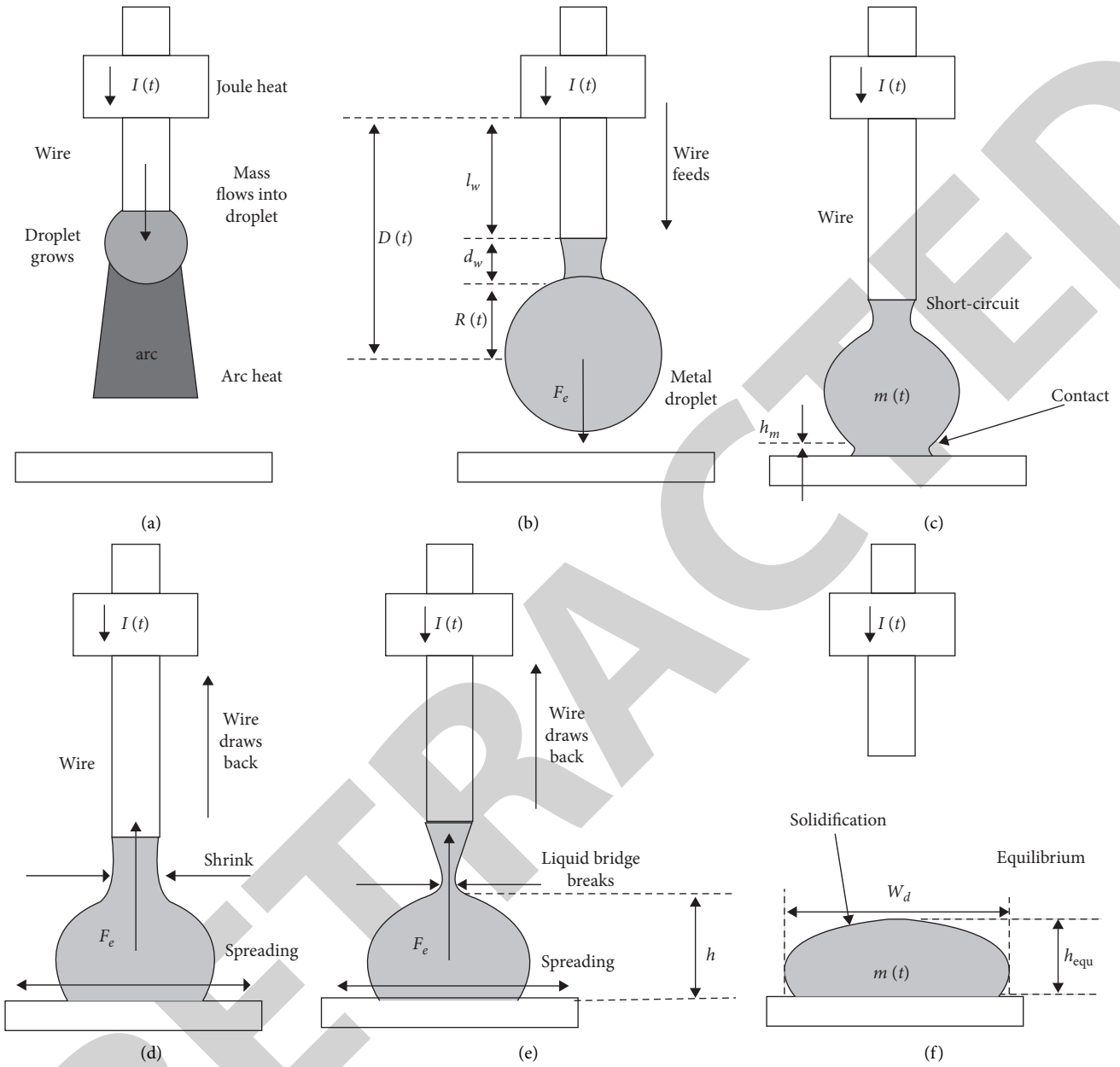
FIGURE 5: Short-circuit transfer model in cold metal transfer.
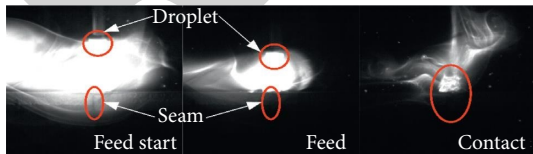
FIGURE 6: Electrode movement in CMT process.

In CMT, the free surface deformation of molten pool is small, the contact interface between droplet and base metal is assumed to be liquid-solid. The metal droplet is difficult to infiltrate the surface of the workpiece, the droplet cannot spread completely over the workpiece and will gradually spread to equilibrium, and the contact angle gradually changes from θ_i to θ_e, as shown in Figure 10.

According to the research by Suli et al. [26], when the droplet impacts with velocity V, the radius of the droplet can be written as

$$\left(\frac{R_B}{R_i}\right)^2 = \frac{(\mathrm{We} + 12)}{3\,(1 - \cos\theta) + 4\,(\mathrm{We}/\sqrt{\mathrm{Ry}})}, \tag{14}$$

where $\mathrm{We} = (\rho R V^2/\gamma)$, $\mathrm{Ry} = (\rho R V/\mu)$, V is the initial velocity of the droplet when it contacts the surface of the molten pool, R_i is the initial radius of the droplet when it comes into contact with the surface of the base material, R_B
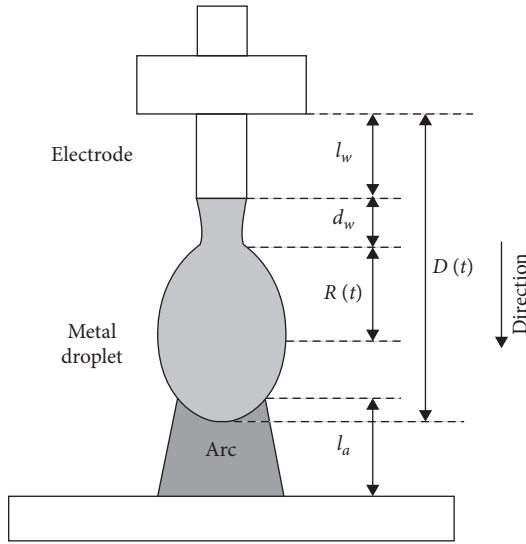
Figure 7: Distance of droplet and workpiece.
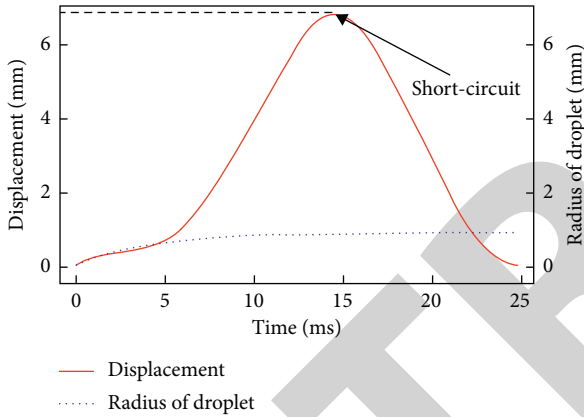
Figure 8: Motion of metal droplet in CMT (wire feed speed is 5.0 m/min).
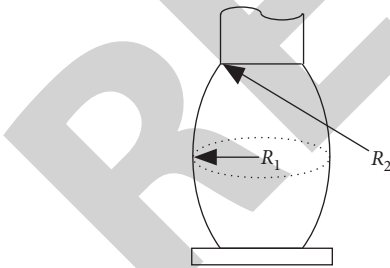
Figure 9: Molten metal bridge.

is the base radius of droplet in spreading process, γ is the surface tension coefficient, and μ is the viscosity coefficient.

Contact angle is expressed as a function of the cosine of the contact angle and time, and is used to describe spreading in reaction-limited wetting:

$$\cos\theta_e - \cos\theta = (\cos\theta_e - \cos\theta_i)\exp(-\lambda t), \quad (15)$$

where θ_i is the initial contact angle, θ_e is the contact angle in equilibrium, and λ is the kinetic constant, assuming that the

kinetic constant does not change with temperature. These values are shown in Table 3.

Equations (14) and (15) lead to the following expression:

$$R_B = R_0 \sqrt{\frac{(We + 12)}{3(1 + (\cos\theta_e - \cos\theta_i)\exp(-\lambda t) - \cos\theta_e) + 4(We/\sqrt{Ry})}}. \quad (16)$$

When the droplet spreads to the equilibrium state, the radius after solidification is the weld width because the droplet solidification time is longer than the spread time.

4. Results and Discussion

During the entire CMT welding cycle, the droplet is formed during the arcing phase, the ends of the wire are melted to form droplets, and the droplet forms a small bridge when in contact with the molten pool. At the same time, the CMT welding obtains a short-circuit signal, then cuts off the current, and the wire is pumped back to help the droplet separate from the electrode.

As shown in Figure 11, the generation of the arc and the growth of the droplet correspond to the arcing phase of the CMT, and the droplet radius increases rapidly. This stage is defined as diffusion. The initial rapid diffusion of droplet is affected by the initial velocity of droplet and the direct heating of arc. This kind of direct arc heating contributes to the rapid diffusion of droplet. At the beginning of the short-circuit transition, the formed droplets are in contact with the electrodes to the surface of the base metal, and are forced to diffuse under the action of inertial forces. This diffusion is affected by surface tension and viscous resistance, and finally reaches equilibrium. When the wire feed speed increases, the welding wire will start to move from a higher distance to the metal surface, the duration of the droplet growth process increases slightly, and the amount of wire metal melted at the end of the wire increases.

The droplet motion is recorded by a high-speed camera, and the contour of the droplet is extracted. The metal transfer and spreading of droplets recorded by the high-speed camera are shown in Figure 12.

Measurements of droplet dimensions are conducted using MATLAB (up to 10,000 frames a test). The program extracts the values of several geometrical characteristics by turning the original image into a binary image. The program is also used to find the edge and calculate the base droplet radius, as shown in Figure 13.

The comparison of the droplet spreading motion with the model calculations shows a better agreement, as shown in Figure 14. The base radius changes very rapidly at the beginning of the spreading. The initial velocity of the droplet transfer to the surface of the sheet is affected by the feed of the wire. After this rapid change, the spreading of the large droplets becomes smoother, and the welding heat is not directly heated by the arc but is conducted through the heat affect zone. According to the spreading dynamics theory, the average expansion speed of metal droplets is lower than the initial phase.

The changes in the base radius at different wire feeding speeds are shown in Figure 15. For thin-plate welding, the change in parameters causes the external force of the droplet
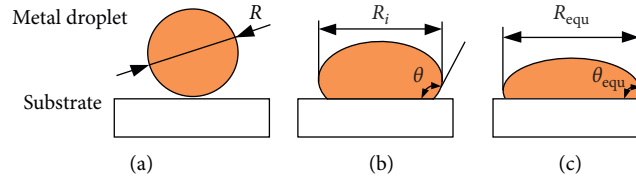
Figure 10: Metal droplet deformation.

Table 3: Physical parameter values used for calculations.

	Properties (units)	Values
θ_i	Initial contact angle (°)	40
θ_e	Contact angle in equilibrium (°)	160
λ	Kinetic constant	20

(a)

(b)
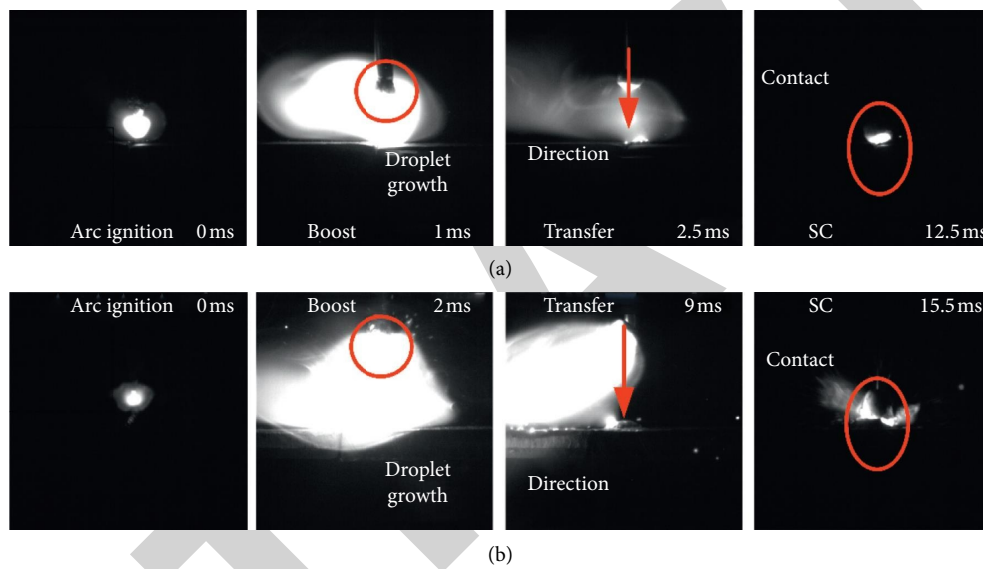
Figure 11: Arc shape and droplet transfer at different process levels: (a) wire feed speed is 3.0 m/min; (b) wire feed speed is 5.0 m/min.
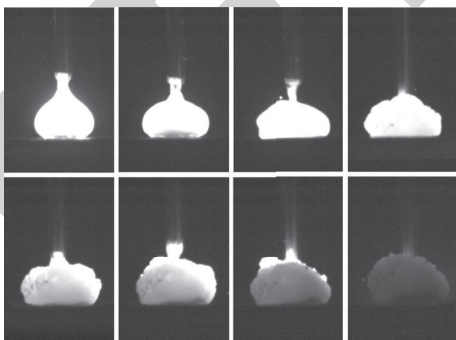
Figure 12: Droplet spreading process (wire feed speed is 5.0 m/min).

Figure 13: Binary image of the droplet radius (wire feed speed is 5.0 m/min).

to change. At the same time, the increase in the current level will change the melting rate of the wire, ensuring that the short-circuit transfer occurs smoothly at a large wire feed speed.

When the wire feeding speed is increased, the molten pool will be affected by the wire movement, thereby increasing the penetration depth and the welding width.

Therefore, in the CMT process, the welding formation is mainly controlled by the movement of the electrode. The droplet transfer is mainly achieved in the form of a short-circuit transition.

The experiment also studied the movement of the droplet under different parameters to verify the versatility and guidance of the theoretical model.

Figure 14: Variation of droplet base radius in spreading stage (wire feed speed is 5.0 m/min).

(a)

(b)
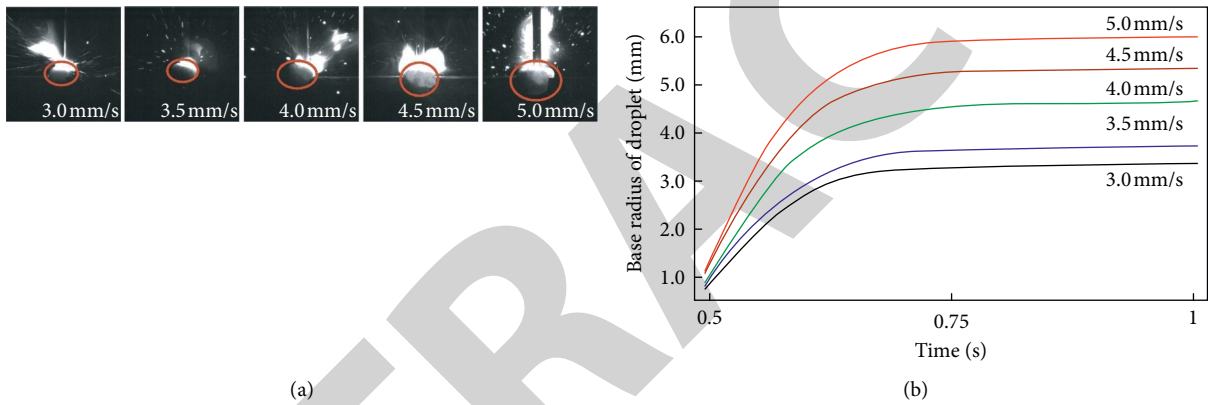
Figure 15: Predictions of the droplet spreading in different wire feed speeds.
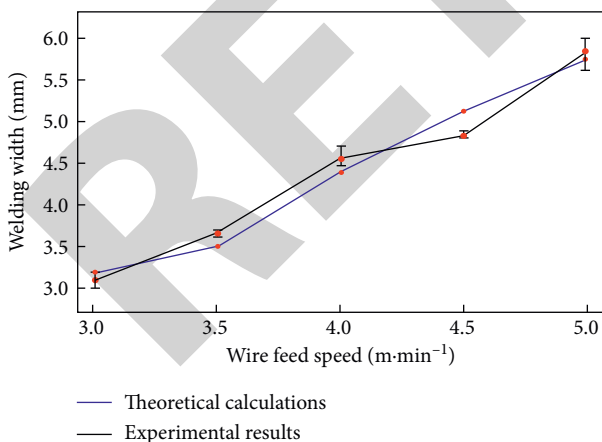
Figure 16: Welding formation in different wire feed speeds.

The model is used to calculate the welding width after droplet spreading and solidification. Figure 16 shows the welding formations in different wire feed speeds. The welding width increases with increasing wire feed speed, and the theoretical calculations show good agreement with the experimental results. In this study, the droplet spreading is 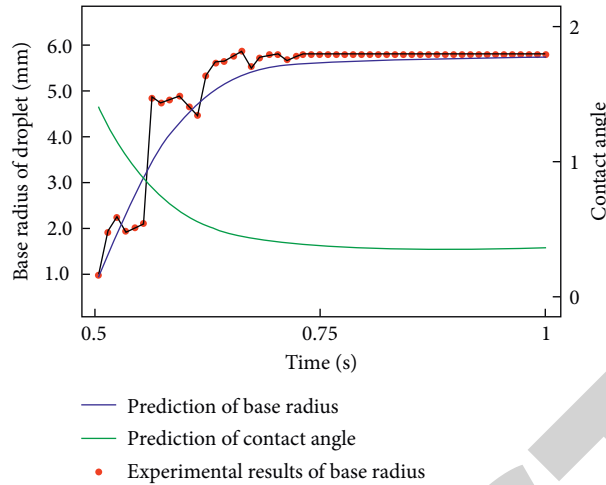considered for the base material with smooth surface, so errors between theoretical calculations and experimental results may exist.

5. Conclusions

A theoretical model of CMT is developed and used to study geometry formation of a droplet during its transfer.

According to the working mechanism of CMT, the influence of CMT pumping motion on wire feeding speed control is analyzed, and the influence of the balance between wire feeding speed and wire melting speed on wire drawing is investigated. Based on wire melting, droplet transfer, and droplet spreading, the droplet movement in CMT welding is analyzed.

Based on the analysis of CMT working mechanism and droplet transfer, the relationship between CMT pumping motion and wire melting rate is considered, the droplet growth and transition model in the CMT working environment is established. Considering the influence of the contact angle on the spreading has been considered, a spreading model of the droplet is established.

The proposed model can effectively predict the motion of droplet in CMT welding and calculate the melting width of the droplet solidified on the base metal.

The theoretical model and the experimental results show a high degree of consistency and can predict the geometry of the weld. This theory allows us to study the motion of this macroscopic droplet in the CMT process.

Abbreviations

k: Boltzmann constant
L: Electrode extension
A: Area of the electrode
Q_J: Joule heat
Q_A: Arc heat
V_a: Arc voltage
Φ: Work function of material
M_R: Wire melting rate
α: Arc heating parameter
β: Joule heating parameter
I: Welding current
l_s: Electrode extension
v_{wfd}:   Wire feed speed
m_R: Droplet mass
$m(t)$:   Droplet mass during droplet transfer period
R: Droplet radius in transfer process
R_i: Initial radius of the droplet when it contacts the surface of base material
R_B: Base radius of droplet in spreading process
R_e: Base radius when the droplet is spread to equilibrium
r: Electrode radius
h_m: Height of meniscus liquid surface
ρ: Mass density
F_e: External forces
μ_0:   Permeability of free space
θ_z: Conduction zone radius
d: Initial distance between the welding wire and the molten pool
$D(t)$:   Displacement of the droplet
l_w: Wire electrode length
d_w: Distance between the droplet and the wire electrode
l_a: Arc length
θ_i: Initial contact angle
θ_e: Contact angle in equilibrium
We: Weber number
Ry: Reynolds number
γ: Surface tension coefficient
μ: Viscosity coefficient.

Data Availability

The data used to support the findings of this study are available from the corresponding author upon request.

Conflicts of Interest

The authors declare that they have no conflicts of interest.

References

[1] B. Wang, S. J. Hu, L. Sun, and T. Freiheit, "Intelligent welding system technologies: state-of-the-art review and perspectives," *Journal of Manufacturing Systems*, vol. 56, pp. 373–391, 2020.

[2] S. B. Chen and N. Lv, "Research evolution on intelligentized technologies for arc welding process," *Journal of Manufacturing Processes*, vol. 16, no. 1, pp. 109–122, 2014.

[3] J. Feng, H. Zhang, and P. He, "The CMT short-circuiting metal transfer process and its use in thin aluminium sheets welding," *Materials & Design*, vol. 30, no. 5, pp. 1850–1852, 2009.

[4] H. Lei, Y. Li, and B. E. Carlson, "Cold metal transfer spot welding of 1 mm thick AA6061-T6," *Journal of Manufacturing Processes*, vol. 28, pp. 209–219, 2017.

[5] R. Cao, G. Yu, J. H. Chen, and P.-C. Wang, "Cold metal transfer joining aluminum alloys-to-galvanized mild steel," *Journal of Materials Processing Technology*, vol. 213, no. 10, pp. 1753–1763, 2013.

[6] R. Cao, Q. Huang, J. H. Chen, and P.-C. Wang, "Cold metal transfer spot plug welding of AA6061-T6-to-galvanized steel for automotive applications," *Journal of Alloys and Compounds*, vol. 585, pp. 622–632, 2014.

[7] P. Wang, S. Hu, J. Shen, and Y. Liang, "Characterization the contribution and limitation of the characteristic processing parameters in cold metal transfer deposition of an Al alloy," *Journal of Materials Processing Technology*, vol. 245, pp. 122–133, 2017.

[8] M. Chen, D. Zhang, and C. Wu, "Current waveform effects on CMT welding of mild steel," *Journal of Materials Processing Technology*, vol. 243, pp. 395–404, 2017.

[9] N. P. Kumar, S. A. Vendan, and N. S. Shanmugam, "Investigations on the parametric effects of cold metal transfer process on the microstructural aspects in AA6061," *Journal of Alloys and Compounds*, vol. 658, pp. 255–264, 2016.

[10] A. B. Murphy, V. Nguyen, Y. Feng, D. G. Thomas, and D. Gunasegaram, "A desktop computer model of the arc, weld pool and workpiece in metal inert gas welding," *Applied Mathematical Modelling*, vol. 44, pp. 91–106, 2017.

[11] H. Komen, M. Shigeta, and M. Tanaka, "Numerical simulation of molten metal droplet transfer and weld pool convection during gas metal arc welding using incompressible smoothed particle hydrodynamics method," *International Journal of Heat and Mass Transfer*, vol. 121, pp. 978–985, 2018.

[12] C. S. Wu, M. A. Chen, and S. K. Li, "Analysis of excited droplet oscillation and detachment in active control of metal transfer," *Computational Materials Science*, vol. 31, no. 1-2, pp. 147–154, 2004.

[13] A. R. Doodman Tipi, S. K. Hosseini Sani, and N. Pariz, "Frequency control of the drop detachment in the automatic GMAW process," *Journal of Materials Processing Technology*, vol. 216, pp. 248–259, 2015.

[14] J. Chapuis, E. Romero, F. Soulié, C. Bordreuil, and G. Fras, "Behaviour of spreading molten metal drops deposited by fusion," *Experimental Thermal and Fluid Science*, vol. 48, pp. 29–36, 2013.

[15] J. Che, S. L. Ceccio, and G. Tryggvason, "Computations of structures formed by the solidification of impinging molten metal drops," *Applied Mathematical Modelling*, vol. 28, no. 1, pp. 127–144, 2004.

[16] S. J. Bless, "Drop transfer in short-circuit welding," *Journal of Physics D: Applied Physics*, vol. 7, no. 4, pp. 526–539, 1974.

[17] U. Ersoy, E. Kannatey-Asibu, and S. J. Hu, "Analytical modeling of metal transfer for GMAW in the globular mode," *Journal of Manufacturing Ence & Engineering*, vol. 130, pp. 551–560, 2008.

[18] M. S. Kang and H. Chung, "Dynamic force balance model considering tapering effect in gas metal arc welding," *Journal of Materials Processing Technology*, vol. 257, pp. 79–87, 2018.

[19] A. Scotti, V. Ponomarev, and W. Lucas, "A scientific application oriented classification for metal transfer modes in GMA welding," *Journal of Materials Processing Technology*, vol. 212, no. 6, pp. 1406–1413, 2012.

[20] J. Huang, W. Pan, W. Yang, C. Xue, Y. Shi, and D. Fan, "The influence of bypass current on metal transfer in dual-bypass gas metal arc welding," *Journal of Manufacturing Processes*, vol. 38, pp. 179–186, 2019.

[21] J.-P. Planckaert, E.-H. Djermoune, D. Brie, F. Briand, and F. Richard, "Modeling of MIG/MAG welding with experimental validation using an active contour algorithm applied on high speed movies," *Applied Mathematical Modelling*, vol. 34, no. 4, pp. 1004–1020, 2010.

[22] J. Norrish and D. Cuiuri, "The controlled short circuit GMAW process: a tutorial," *Journal of Manufacturing Processes*, vol. 16, no. 1, pp. 86–92, 2014.

[23] J. Pang, S. Hu, J. Shen, P. Wang, and Y. Liang, "Arc characteristics and metal transfer behavior of CMT + P welding process," *Journal of Materials Processing Technology*, vol. 238, pp. 212–217, 2016.

[24] P. J. Modenesi and R. I. Reis, "A model for melting rate phenomena in GMA welding," *Journal of Materials Processing Technology*, vol. 189, no. 1–3, pp. 199–205, 2007.

[25] D. Sivakumar and H. Nishiyama, "Spreading and solidification of a molten metal droplet impinging on a heated surface," *International Journal of Heat and Mass Transfer*, vol. 47, no. 19-20, pp. 4469–4478, 2004.

[26] S. Li, W. Liu, L. Yang et al., "Building 3D parts based on metal droplet deposition process," *Rare Metal Materials and Engineering*, vol. 48, pp. 626–631, 2019.